Direct Electrografting of Poly(2-alkyl-2-oxazoline)s on Gold, ITO, and Gold Nanoparticles for Biopassivation

Dihia Benaoudia, Van-Quynh Nguyen, Véronique Bennevault, Pascal Martin, Fabien Montel, Philippe Guégan,* and Jean-Christophe Lacroix*

Cite This: https://doi.org/10.1021/acsanm.3c02379

Read Online

| ACCESS | | Metrics & More | | Article Recommendations | | Supporting Information |

ABSTRACT: Poly(2-alkyl-2-oxazoline)s (POx) bearing an aminophenyl end group were synthesized by cationic ring-opening polymerization; the polymers were then carefully characterized by NMR, size exclusion chromatography, and differential scanning nano calorimetry. The electroreduction of the diazonium salts of aniline terminated poly(2-methyl-2-oxazoline) (PMeOx) and poly(2-n-propyl-2-oxazoline) (PnPrOx) from aqueous solution on indium tin oxide (ITO) and gold (Au) and through a two-dimensional polystyrene (PS) template has been investigated. On all substrates, ultrathin layers of polymer are grafted and deposited. Modified surfaces were characterized by electrochemistry, scanning electron microscopy (SEM), X-ray photoelectron spectroscopy (XPS), and atomic force microscopy. Nanoporous honeycomb POx structures have been obtained thanks to electrochemical growth in the interstitial spaces between self-assembled PS spheres. Finally, the wettability of the surfaces depends markedly on the chemical nature of the POx, with contact angles of 32° and 70° for modified surfaces with PMeOx and PnPrOx.

KEYWORDS: surface functionalization, cationic ring-opening polymerization, diazonium salt reduction, poly(2-oxazoline)s, smart surface
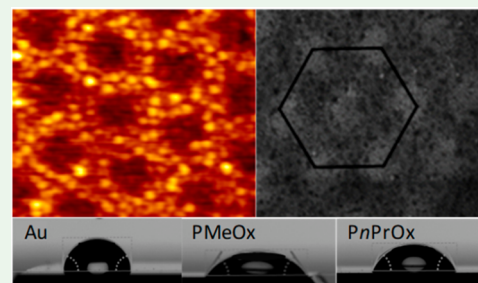
INTRODUCTION

Surface modification has been widely addressed in corrosion protection[1−3] smart coatings,[4−7] and sensing and biomedical applications.[8−10] Adsorption of thiol−organic compounds onto a gold surface was revealed to be an easy strategy to form self-assembled monolayers that could be the base for further building more complex structures[11,12] This easy process is however hampered by the poor stability of such layers in harsh conditions, especially in oxidative or reductive media.[13] In the case of SiO_2 surface, the silane chemistry is the most common process used.[14,15] Both chemistries have been extended to other metal and oxide surfaces modifications. Grafting a poly(aryl)-based layer using diazonium salt reduction is another strategy that could be used for surface modification of many substrates (metallic, semiconducting, polymer, diamond, carbon nanotubes, ...).[16−18] This grafting chemistry relies on the formation of aryl radical from diazophenyl derivatives, able then to react with any surface. Formation of the aryl radical was first ensured by electroreduction[16,17] but it was later shown that ultrasonic, UV and visible light could also be used to generate the reactive phenyl radical.[19−21] This grafting chemistry offers an ease of preparation, a large choice of available reactive functional groups, and a strong aryl−surface bonding. The structure of the aryl film can, however, be complex: the reactive aryl radical reacts on the surface but also on the first grafted aryl residues. The resulting organic layer is then composed of many aryl

layers with total film thickness ranging from few nm, when the deposited film is insulating,[22,23] to μm when it incorporates redox active groups acting as electronic relay during electrochemical reduction.[24−26] Several strategies have been proposed to limit the growth of multilayers. Among them are the use of sterically hindered aryl derivatives, such as 3,5-bis-*tert*-butyl benzenediazonium salts,[27] and of diazonium salts derived from inorganic complexes[28] or bearing bulky protective groups[29] and the use of ionic liquids[30] or of radical scavengers.[31−33]

Grafting saturated polymers on surfaces is an important coating strategy for controlled wettability, chelating surfaces, molecular imprinted polymer grafts, protective issue of the surface, and biopassivation.[34−36] This last notion covers antifouling properties,[37] antibacterial properties,[38] corrosion inhibition by biofilms[39] and nonspecific adsorption of biological molecules of various molar masses onto surfaces.[40] Polymer chemisorption, i.e., the grafting of a polymer chain on a surface via a covalent bond, has been found to be more resistant than physisorption, and the grafting can be ensured via various strategies: a "grafting from" strategy consisting of a

polymerization of a monomer from a small initiator already grafted on the surface or a "grafting onto" method issued from the grafting of a premade polymer onto a surface via a chemical reaction. The "grafting from" method requires an efficient initiation reaction with a fast kinetics of the propagating step that essentially limits the polymer "grafting from" approach to radical chemistry. In this respect, most of the work dedicated to formation of polymeric monolayer on a surface using the diazonium salt chemistry relies on building a first functional aryl layer on which initiation functions are grafted to start the growing of polymer chains from the surface.[41,42] Grafting brominated aryl layers on surfaces enabled the use of atom transfer radical polymerization to control the molar mass of the grafted polymer layers and to provide very dense polymer layers.[43,44] This grafting strategy was for example applied to methacrylate, N-isopropylacrylamide, vinylpyridine or styrene monomers.[45] Homopolymer grafts from R-*tert*-butoxy-ω-vinyl-benzylpolyglycidol (PGL) were prepared on gold and stainless-steel substrates modified by 4-benzoylphenyl moieties derived from the electroreduction of the parent salt 4-benzoylbenzene diazonium tetrafluoroborate.

Grafting onto is an alternative strategy in which a first aryl layer bearing various coupling groups is deposited on a surface, and a premade polymer is attached on this layer in a second step. Several examples can be found in the literature. The attachment of carboxyphenyl groups to the iron surface by reduction of the diazonium salt of 4-aminobenzoic acid and the further attachment of poly(1,2-propanediyl fumarate) to the phenylcarboxylate functions through ionic bonds with Mg^{2+} ions was reported 30 years ago.[46] *Clicking* macromolecules to grafted diazonium salt-derived aryl layers was shown to be a simple and valuable approach for designing robust, functional surface organic coatings.[47] Grafting long polyethylene glycol (PEG) oligomers or commercial surfactants by a reaction of the linear polymer with a premade aryl layer was recently reported.[48] Functional polymers bearing a diazonium terminal group have also been synthesized and then grafted onto the surface. Low molar masses oligomers of tetra(ethylene oxide) derivatives have been used with this coupling chemistry[49] in order to generate surface modulation of single-walled carbon nanotubes for selective bacterial cell agglutination.

Polypyrrolidone, polyglycidol, or poly(2-alkyl-2-oxazoline) have recently been proposed to replace PEG for various reasons ranging from better fouling properties[50−52] to higher biocompatibility.[53,54] Poly(2-alkyl-2-oxazoline) was recently widely developed for biological applications, and it revealed a high potential for PEG substitution in every application related to medical science and surface coating.[55]

Grafting from polymerization of 2-ethyl-2-oxazoline on a surface was reported by Jordan *et al.* as early as 1998.[56,57] The initiator was first linked to the surface using the thiol-gold chemistry, and then grafting from polymerization of 2-ethyl-2-oxazoline was conducted to provide a polymer monolayer with a high estimated grafting density. Linear or cyclic poly(2-alkyl-2-oxazoline)s were grafted onto surfaces using thiol chemistry[58,59] or polyelectrostatic interactions.[60]

Quite large molar masses of poly(2-alkyl-2-oxazoline) could be grafted on various surfaces; however, the long-term robustness of the anchoring could be questioned. Surprisingly, the grafting of poly(2-alkyl-2-oxazoline) from polymers bearing diazonium end groups has never been reported, while this versatile strategy represents an original way to coat any surface by polymers through a robust aryl covalent anchor.

In the present work, we will first describe the one-pot synthesis of aniline end-functionalized poly(2-alkyl-2-oxazoline)s thanks to a controlled termination reaction between 1-(4-aminophenyl)piperazine and the oxazolinium function of the growing polyoxazoline chains. This reaction will be investigated for two series of oxazoline monomers, i.e. 2-methyl-2-oxazoline (MeOx) and 2-n-propyl-2-oxazoline (n-PrOx). Then grafting of the polymers on a gold surface using the electroreduction of *in situ* formed diazonium reactive functions from the terminal aminophenyl groups born by the polymers with various molar masses was studied (Figure 1). The effect of the lower critical solution temperature (LCST) of poly(2-n-propyl-2-oxazoline) onto the grafted polymer layer will be investigated.
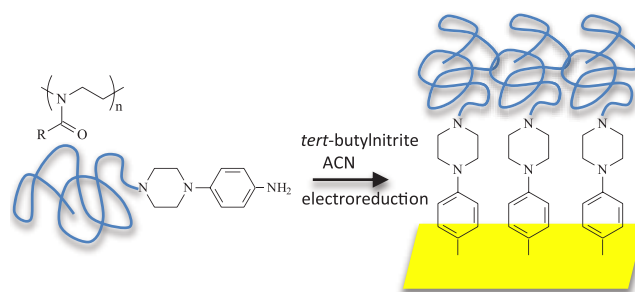
Figure 1. Electrografting of poly(2-alkyl-2-oxazoline) layer on a gold surface.

RESULTS AND DISCUSSION

Synthesis of PMeOx and PnPrOx. Oxazoline monomers were polymerized in acetonitrile at 80 °C, conditions that were reported to provide controlled polymerizations.[61−63] Allyl bromide was selected as the initiator in order to enable a fast and complete initiation reaction (Figure 2). For all of the
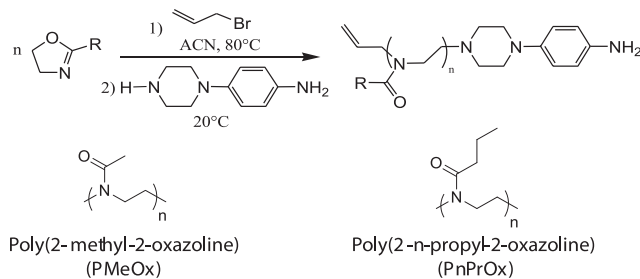
Figure 2. Cationic ring-opening polymerization of 2-alkyl-2-oxazolines (MeOx or n-PrOx).

experiments, targeted degrees of polymerization (X_n) were calculated from initial molar concentration ratio $[M]_0/[A]_0$ and were deliberately set between 30 and 60. Quantitative initiation was assumed. So chain ends could be easily characterized by ^1H NMR for the termination reaction investigation. 1-(4-aminophenyl)piperazine was selected as the terminating agent to provide poly(2-alkyl-2-oxazoline)s with aminophenyl chain-ends. Assumption was made the secondary amino function of the piperazine derivative would react much faster than the aniline function with the oxazolinium growing chain ends.

First, polymerizations of MeOx were conducted for 24 h at 80 °C (Table 1), and the termination time by 1-(4-

Table 1. Experimental Conditions and Molecular Characteristics of PMeOx

Run[a]	$[M]_0/[A]_0/[Q]_0$[b]	Convn[c] (%)	$X_{n\ th}$[d]	$X_{n\ NMR}$[e]	$X_{n\ SEC}$[f]	Đ[f]	F[g] (%)	Diff. Coeff[h] (m²·s⁻¹)
1	60/1/1.2	98	58	95	81	1.26	46	$(2.2 \pm 0.1) \times 10^{-10}$
2	55/1/5	99	54	66	64	1.25	79	$(2.0 \pm 0.1) \times 10^{-10}$

[a]Solvent: ACN. Temperature: 80 °C. Termination time: 66 h. [b][A]₀, [M]₀, [Q]₀: respectively initial initiator, monomer, and terminating agent concentration, $[M]_0$ = 1.5 mol·L⁻¹, [c]Monomer conversion determined from the medium reaction by ¹H NMR in CDCl₃, [d]$X_{n\ th}$ = [M]₀ × Convn/[A]₀, [e]Determined by ¹H NMR from allyl end chains, [f]Determined by SEC (DMF, 60 °C, PMMA standards), [g]Functionalization ratio determined by ¹H NMR, [h]Diffusion coefficient determined by DOSY NMR.

Table 2. Experimental Conditions and Molecular Characteristics of PnPrOx

Run[a]	$[M]_0/[A]_0/[Q]_0$[b]	t_{polym}[c] (h)	Convn[d](%)	$X_{n\ th}$[e]	$X_{n\ NMR}$[f]	$X_{n\ SEC}$[g]	Đ[g]	F[h] (%)	Diff. Coeff[i] (m²·s⁻¹)	LCST (°C)
3	32/1/5	24	94	30	48	64	1.06	95	$(1.94 \pm 0.04) \times 10^{-10}$	23
4	40/1/5	48	98	39	40	38	1.10	100	$(2.42 \pm 0.06) \times 10^{-10}$	26

[a]Solvent: ACN. Temperature: 80 °C. Termination time: 66 h. [b][A]₀, [M]₀, [Q]₀: respectively initial initiator, monomer and terminating agent concentration, $[M]_0$ = 1.5 mol·L⁻¹, [c]Polymerization time. [d]Monomer conversion determined from the medium reaction by ¹H NMR in CDCl₃. [e]$X_{n\ th}$ = [M]₀ × Convn/[A]₀. [f]Determined by ¹H NMR from allyl end chains. [g]Determined by SEC (DMF, 60 °C, PMMA standards). [h]functionnalization ratio determined by ¹H NMR. [i]Diffusion coefficient determined by DOSY NMR.
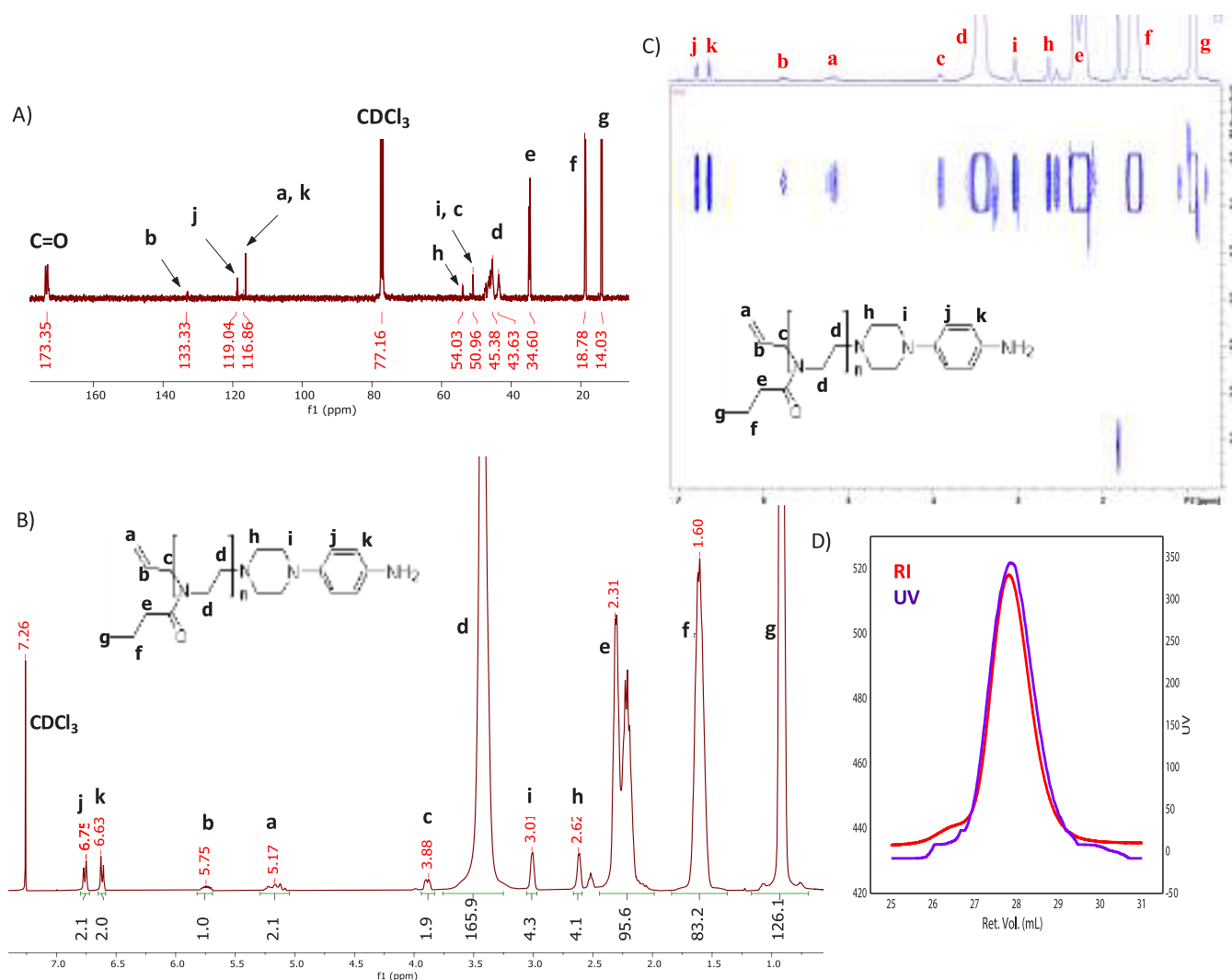
Figure 3. PnPrOX (Table 2, run 4): (A) ¹³C and (B) ¹H NMR spectra in CDCl₃ at 20 °C, (C) DOSY NMR spectrum in CDCl3 at 298 K, and (D) SEC trace: RI (red), UV (purple) at λ = 254 nm.

aminophenyl)piperazine was set to 66 h, with a terminating agent/initiator ratio between 1.2 and 5. NMR analyses of the reaction media revealed a complete monomer conversion within 24 h. Using the unsaturation signal at 5.23 ppm

witnessing the allyl end chains and the monomer unit signal at 3.44 ppm, the NMR degrees of polymerization were determined on the purified polymers spectra. The functionality of the polymers was calculated comparing the intensity of the

piperazine cycle methylene protons at 3.05 and 2.66 ppm and the intensity of the unsaturated protons at 5.80 ppm. In our first trial, the conditions used (1.2 eq. of terminating agent/initiator) led to only 46% of functionalization by the aminophenyl group (run 1), while a terminating agent/initiator ratio equal to 5 enabled to obtain a functionality equal to 79% (run 2). Nevertheless, this rate is sufficient for the targeted application, since after the grafting step, the surface was washed, suppressing the nonfunctionalized chains. The chemical structure of the synthesized polymers was confirmed by 1D (Figure S1) and 2D NMR analyses (COSY, HSQC and DOSY NMR, Figures S2−S4). The DOSY experiments showed the covalent bond between the polymer and the piperazine derivative, since all the NMR signals broadcasted at the same speed. The polymers had diffusion coefficients (Table 1) in the range 2×10^{-10} m$^2 \cdot$s^{-1} that were much lower than the value determined in the same conditions for 1-(4-aminophenyl)piperazine. The latter was equal to $(1.34 \pm 0.01) \times 10^{-9}$ m$^2 \cdot$s^{-1}. The functionalization of the chains was also highlighted by Size Exclusion Chromatography (SEC), since an overlap of the RI and UV signals was observed (Figure S5). This result indicated that all of the chains contained a piperazine group. However, the SEC chromatograms showed a shoulder toward low elution volume, whose intensity increased with decreasing terminating agent/initiator ratio. The molar mass of this population was twice as high as the main population one. These results suggest that a small fraction of growing chains is deactivated by both the piperazine and aniline end chains of 1-(4-aminophenyl)piperazine. Note that these chains are eliminated during washing of the grafted surface. This issue is solved by increasing the excess of the terminating agent. With an excess of 5 (Table 1, run 2), the degrees of polymerization determined by SEC and NMR are in good agreement with the theoretical value. Moreover, Figure S6 reports polymerizations conducted with 10 equiv of terminating agents, and the shoulder at low elution volume disappeared on the SEC analysis, witnessing the expected functionalization.

A ratio of $[Q]_0/[A]_0$ equal to 5 was used to synthesize poly(2-n-propyl-2-oxazoline)s (PnPrOx). Data are listed in Table 2. The structure of the polymers was confirmed by NMR (Figure 3A,B and Figures S7 and S8). Once again, the covalent bond between the polymer chain and terminating agent was highlighted by SEC (Figure 3D) and by the measurement of the diffusion coefficients by DOSY NMR (Figure 3C). In this set of experiments, an excess of terminating agent equal to 5 was sufficient to obtain a complete functionalization of the chains during the termination step and no shoulder was observed in the SEC chromatograms, suggesting a high control of the polymers structure. This point is in agreement with the lower dispersities and the lower standard deviations of diffusion coefficients obtained in SEC and NMR (Table 2). This kind of polymers is known to have a lower critical solution temperature. The LCST values determined by nanoDSC are about 25 °C ([PnPrOx] = 5 mg/mL). A small variation was noted according to the degree of polymerization of the sample ($X_{n\ SEC}$ = 38 or 64). The values obtained in this study are close to the published values.[64,65] For example, a LSCT of 30 °C was mentioned for a polymer with methyl and alcohol end-chains and with a X_n equal to 60.[64] The more hydrophobic aminophenyl group induced a slight decrease in the LCST value in the present case.

Electrografting. PMeOx was grafted by the electrochemical reduction of diazonium salts on various electrodes (gold, ITO, and ITO bearing gold nanotriangles). As an example, Figure S9 shows the electrochemical grafting performed in acetonitrile by cyclic voltammetry. The diazonium salt was generated *in situ* from PMeOx-aminophenyl in the presence of tBuNO$_2$. The recorded CV displays irreversible reduction waves at −0.09 V and a broad reduction current from 0.3 to −0.8 V, associated with the reduction of PMeOx diazonium. During subsequent cycles, the intensity of the cathodic current decreases. Similar behavior has been observed during the reduction of *in situ* generated aryldiazonium cations.[66] This behavior is attributed to the progressive modification of the electrode by the formation of an insulating organic film, which partially blocks the surface in the 0.45 to −0.8 V potential range. The electrochemical reduction of the other polymers PnPrOx behaves similarly.

The blocking effect of the deposited layer was investigated by using redox probes in solution. The voltammogram of Ferrocene (Fc) in ACN solution on ITO electrode was recorded (Figure 4) before (black) and after (red) PMeOx
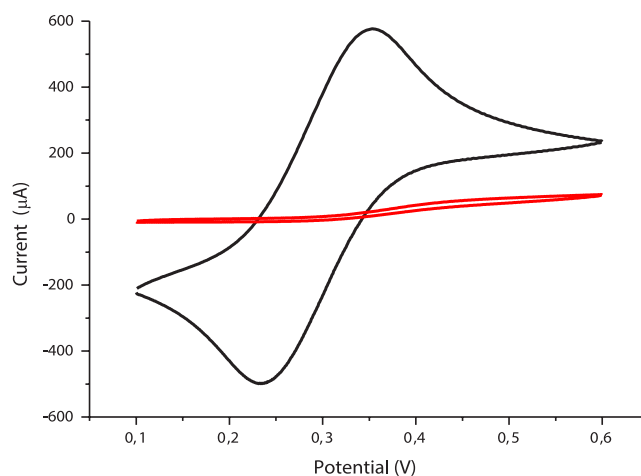
Figure 4. CVs of ferrocene (10^{-3} M in acetonitrile with 0.1 M LiClO$_4$) at 100 mV·s^{-1} before (black curve) and after (red curve) grafting of PMeOx (run 2, Table 1) on ITO electrode.

electrografting. A strong decrease in the current of ferrocene is observed on the modified ITO electrode. This confirms that a compact film, with a large surface coverage and few micrometric holes, has been deposited on all the ITO surface which is covered by the polymer.[67] The surface was also dipped in ACN after grafting for 30 min to try to remove the physiosorbed polymer from the surface and characterized again. The electrochemical signal of ferrocene remained close to that of Figure 4 (red curve) which shows that the film is robustly attached to the surface.

XPS analysis was also used to analyze the surface composition of the generated film. To do so, we deposited the various films on a 1 cm^2 gold electrode.

Figure 5 displays the high-resolution XPS signal for Au 4f (peaks around 84 and 88 eV Figure 5a) and the high-resolution XPS signal for N 1s (peak around 400 eV Figure 5b) obtained on the Au modified surface. Several major differences can be observed in the XPS spectra before and after electrochemical grafting. First, the gold signal decreases after the reduction of diazonium, in comparison with the bare
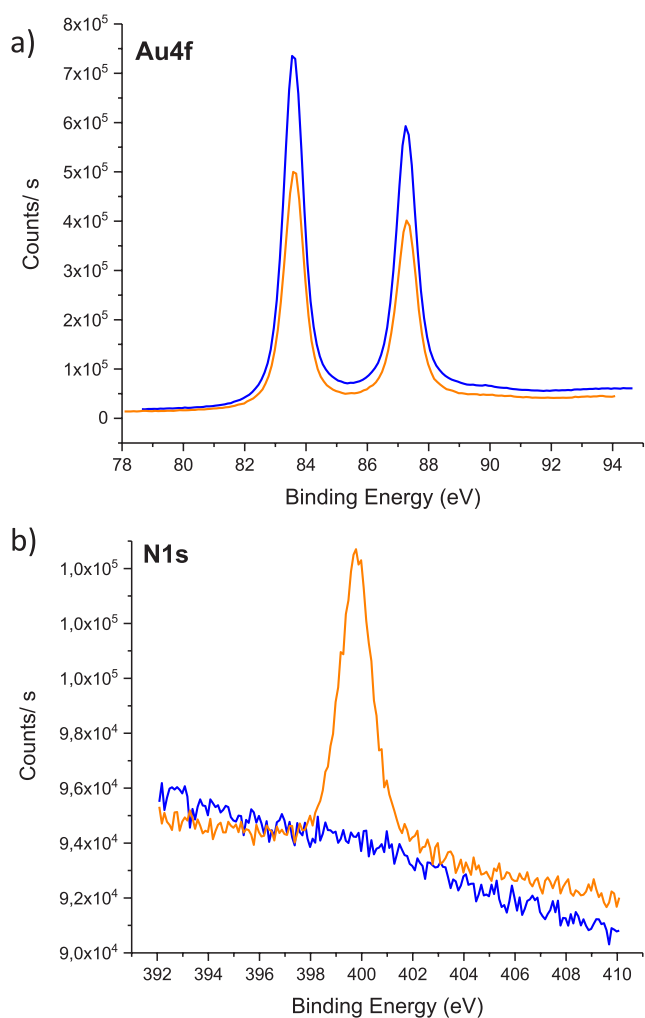
Figure 5. High-resolution XPS spectra of a gold surface before (blue) and after (orange) PMeOx (run 2, Table 1) electrografting: (a) high resolution Au 4f signals and (b) high resolution N 1s signal

deposited on a ITO surface using an already published procedure.[6] PMeOx diazonium salt electroreduction was then performed on these nanostructured electrodes, and grafting was confined in the free space between adjacent nanospheres. PS Spheres were then removed in THF under ultrasonic conditions, and the generated surface was studied by SEM and AFM. Figure 6 shows that the surface consists of a nanohole
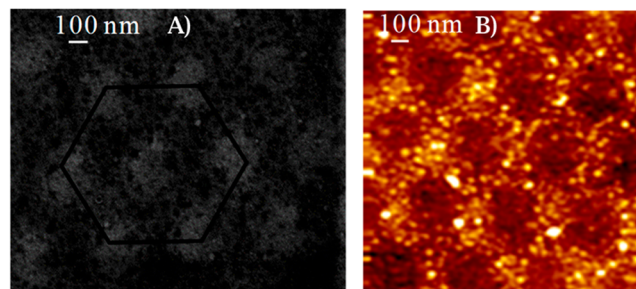
Figure 6. (A) SEM image. (B) AFM image of nano structured array of a PMeOx (run 2, Table 1) layer on ITO obtained using a 500 nm diameter PS sphere.

substrate, which indicates the formation of an organic layer. Second, the detection of the Au XPS signals, in the survey spectrum is an indication of rather thin film, below 10 nm. Third a nitrogen signal appears after polymer deposition.

Table 3 summarizes the experimental and theoretical ratios of the different elements observed on the grafted surface. The

Table 3. Summary of XPS Results

ratio	theoretical	experimental
O/N	0.96	0.94
O/C	0.05	0.03
N/C	0.17	0.15

ratio O/N found by XPS analysis (0.94) is in very good agreement with the theoretical composition of PMeOx if immobilized on the surface (0.96). N/C and O/C ratios are also in very good agreement with theoretical ratios, which confirms that a thin film of PMeOx is grafted on the gold surface.

Measuring the thickness of such film is not easy and was done, in this study using nanosphere lithography combined with PMeOx diazonium salt electroreduction.[68] A monolayer of polystyrene (PS) spheres (500 nm diameter) was first

array hexagonally organized on a large area. Indeed, after the removal of the spheres, the SEM image shows white circular spots, organized in a honeycomb arrangement, within dark areas. The apparent diameter of each white spot is 200 nm, corresponding to the area previously occupied by the PS spheres. The center-to-center distance between two adjacent circular spots is 500 nm and corresponds to the diameter of the spheres used. This clearly confirms that the spheres are close-packed, with an organized 2D layer acting as a mask for diazonium electroreduction. The surfaces after bead dissolution consist clearly of a hexagonal organization of nanometric holes in a layer of grafted poly(2-methyl-2-oxazoline)s. Free ITO areas are clearly visualized as white spots in the SEM image of the modified surface.

The topology and morphology of the nanostructure on the ITO surface were further characterized by AFM (Figure 6B). Holes in the PMeOx layer are now seen as dark spots and the honeycomb arrangement in nanohole arrays is clearly observed. The AFM topographies exhibit brighter areas where PMeOx grafting took place and show a local morphology with small protuberance likely indicating that the grafted polymer self-aggregates which yields to a high local roughness when compared to modified surface obtained after diazonium grafting using smaller molecules.[25,28] Figure S10 shows an AFM image of a larger area along with the line profile. It shows an average hole height between 3 and 5 nm and confirms that the PMeox film is ultrathin and that due to the steric hindrance of the long polymer chains, thick multilayers are not obtained. Note also that thicknesses measured by AFM are coherent with those deduced from the Au XPS signal. Next, the contact angles of water on various PMeOx and PnPrOx modified gold electrodes, generated by cyclic voltammetry were measured and compared. Films generated from PMeOx-aminophenyl, runs 1 and 2 (Table 1), in the presence of tBuNO$_2$ in ACN are characterized by water contact angles of 32° and 55°, respectively, i.e., smaller than the 83° contact angle measured on the Au bare surface. PMeOx modified surfaces are thus more hydrophilic than bare gold because of the hydrosoluble properties of the grafted polymer and increasing the chain length (between run 1 and

run 2) decreases the contact angle. On P*n*PrOx-Au modified surface reaches 70° (Figure 7). These results are in good

Figure 7. Wettability of (a) Au surface, (b) Au modified by PMeOx (run 2, Table 1), and (c) Au modified by PnPrOx (run 4, Table 2)

agreement with the chemical proprieties of poly(2-alkyl-2-oxazoline)s as it is known that P*n*PrOx is less hydrophilic than PMeOx. Overall, the variations of the contact angles after the electrografting process indicate that the hydrophilic polymers are grafted on the surface.

Finally, PMeOx was also grafted on arrays of gold triangles deposited by nanosphere lithography on ITO. SEM image of such substrates are given as Figure S11. These substrates show a localized surface plasmon resonance (LSPR) at 800 nm. The wavelength of such LSPR is known to be highly sensitive to the surrounding medium with a red shift when an organic material with a dielectric constant above 1 is deposited on the nanotriangles. Figure S12 shows that upon PMeOx electrografting the LSPR of the gold nanotriangle red shift from 824 to 854 nm which again clearly demonstrates that an organic layer has been deposited on the gold Nps.[20,69]

CONCLUSION

Several poly(2-alkyl-2-oxazoline)s bearing an aminophenyl end group were synthesized by cationic ring-opening polymerization and carefully characterized. The electrografting of these polymers in acetonitrile solution on indium tin oxide (ITO), gold (Au), through a two-dimensional polystyrene (PS) template or on ITO bearing gold nanotriangles (AuNPs) were demonstrated. On all substrates, ultrathin layers of polymer are obtained. Nanoporous honeycomb POx structures have been obtained thanks to the electrochemical growth in the interstitial spaces between self-assembled PS sphere. The effect of POx grafting on the plasmonic properties of AuNPs was reported, and the wettability of the surfaces was shown to markedly depend on the chemical nature of the POx. For a more general point of view, this study demonstrates that surfaces modified by poly(2-alkyl-2-oxazoline) can be easily obtained, which could be of tremendous interest in order to replace PEG coatings for various applications using biocompatible surfaces.

EXPERIMENTAL SECTION

1. Materials. 2-Methyl-2-oxazoline (98%, Aldrich), 2-*n*-propyl-2-oxazoline (98%, TCI), allyl bromide (97%, Aldrich), and acetonitrile (VWR) were purified by refluxing over calcium hydride under nitrogen and distilled before use. 1-(4-Aminophenyl)piperazine (97%, Aldrich), *N*-dimethylformamide (anhydrous, 99.8%, Aldrich), and methanol were used without further purification. Deuterated chloroform was purchased from Euriso-TOP. Dialysis membranes used were Biotech Cellulose Ester membranes with a 500 Da cutoff pore size (Spectrum Laboratories).

2. Instruments. *NMR Spectroscopy.* ^{1}H and ^{13}C NMR analyses were conducted on a Bruker Avance 300 or 400 MHz spectrometer. All spectra are internally referenced to residual proton signals of the deuterated solvent ($CDCl_3$). The Diffusion-Ordered SpectroscopY (DOSY) experiments were carried out at 298 K on a 400 MHz spectrometer using the ledbpgp2s.mod pulse sequence with a linear gradient of 16 steps between 5% and 95%. The maximum field

gradient strength was equal to 5.54 G.mm⁻¹. Before each diffusion experiment, the length of the gradient δ and the diffusion time Δ were optimized. The software used for data analysis was Topspin. The used mathematical treatment of the data was previously described.[70]

Size Exclusion Chromatography (SEC). Polymer molar masses were determined by SEC using DMF containing 1 g·L⁻¹ lithium bromide as already reported.[71] The OmniSEC 4.6.2 software was used for data acquisition and data analysis. The number-average molar masses (M_n), the weight-average molar masses (M_w), and dispersity ($Đ = M_w/M_n$) were determined with a calibration curve based on narrow poly(methyl methacrylate) (PMMA) standards (from Polymer Standard Services), using the RI detector.

Nano DSC. Thermograms were measured using an N-DSC III instrument from TA Instruments. The reference cell was filled with water, and the sample cell (0.3 mL) was filled with the polymer solution. The capillary cells were not capped, and a constant pressure of 6×10^5 Pa was applied. A baseline scan (solvent in both reference and sample cells) was systematically performed under identical conditions and subtracted from the sample scan. The transition temperature was measured as the average of heating and cooling scans, at a scan rate of 1 °C·min⁻¹.

XPS Analysis. XPS analysis was performed using Kratos AXIS XPS with Al Kα radiation and depth profiling with a 4 kV Ar⁺ beam at 5×10^{-10} Torr. Deposition of PMeOx and P*n*PrOx layers was achieved using the same procedure as that cited before. Survey and high-resolution spectra for C, N, O, and Au were obtained initially and after polymers grafting. CasaXPS software was used for deconvolution of the XPS spectra using a Shirley baseline and Gaussian−Lorentzian line shapes.

Localized Surface Plasmon Resonance (LSPR). Extinction measurements were carried out with an Ocean Optics HR 4000 UV−vis spectrophotometer (optical resolution: 0.3 nm) coupled with a fiber-optic system which made it possible to analyze an area of 80 μm × 80 μm.

3. Polymerizations of 2-Methyl-2-oxazoline and 2-*n*-Propyl-2-oxazoline. PMeOx and P*n*PrOx were synthesized via cationic ring-opening polymerization using the same operating conditions: polymerizations were carried in acetonitrile (ACN) at 80 °C under nitrogen, and the initial monomer concentration was set to 1.5 mol·L⁻¹. The procedure was detailed for run 2 of Table 1. In a glovebox under a nitrogen atmosphere, 20 μL (2.31×10^{-4} mol, 1 equiv) of allyl bromide, 7.4 mL of ACN, and 1.08 mL (1.27×10^{-2} mol, 55 equiv) of MeOx were successively introduced into a Schlenk flask equipped with a magnetic stirrer. The polymerization was stirred at 80 °C for 24 h and then quenched at room temperature by adding an excess of 1-(4-aminophenyl)piperazine (205 mg, 1.16×10^{-3} mol, 5 equiv, dissolved in 3 mL of ACN). The mixture was stirred for 66 h. The solvent was then evaporated and the polymer was dried in vacuum overnight at 50 °C, yielding a solid product. This product was solubilized in methanol and dialyzed against methanol for 8 h to remove the terminating agent excess. The monomer conversion was determined from the reaction medium before the solvent elimination by ^{1}H NMR spectroscopy, while molar masses were determined from purified polymer by SEC and ^{1}H NMR.

4. Other. Atomic force microscopy, SEM characterization, elaboration of the polystyrene nanosphere mask for nanosphere lithography, and electrografting of the organic layers have been extensively described in previous publications.[6,68,72] Figure S13 shows the chemical reaction leading to a diazonium salt from an aromatic amine reacting on tBuNO₂.

ASSOCIATED CONTENT

ⓢ Supporting Information

The Supporting Information is available free of charge at https://pubs.acs.org/doi/10.1021/acsanm.3c02379.

> 2D NMR analyses (COSY, HSQC and DOSY NMR), Size Exclusion Chromatography (SEC) of the generated polymers, SEM image of a plasmonic electrode bearing gold nanotriangles deposited by nanosphere lithography,

Extinction spectra of the plasmonic electrode before and after PMeOx elecrochemical grafting (PDF)

AUTHOR INFORMATION

Corresponding Authors

Philippe Guégan − *Equipe Chimie des Polymères, Institut Parisien de Chimie Moléculaire, Sorbonne Université, CNRS, F-75005 Paris, France;* orcid.org/0000-0002-4919-0779; Email: Philippe.guegan@sorbonne-universite.fr

Jean-Christophe Lacroix − *Université Paris Cité, ITODYS, UMR 7086 CNRS, F-75205 Paris Cedex 13, France;* orcid.org/0000-0002-7024-4452; Email: lacroix@univ-paris-diderot.fr

Authors

Dihia Benaoudia − *Université Paris Cité, ITODYS, UMR 7086 CNRS, F-75205 Paris Cedex 13, France; Equipe Chimie des Polymères, Institut Parisien de Chimie Moléculaire, Sorbonne Université, CNRS, F-75005 Paris, France*

Van-Quynh Nguyen − *Université Paris Cité, ITODYS, UMR 7086 CNRS, F-75205 Paris Cedex 13, France; Department of Advanced Materials Science and Nanotechnology, University of Science and Technology of Hanoi (USTH), Vietnam Academy of Science and Technology, 11307 Cau Giay, Hanoi, Vietnam*

Véronique Bennevault − *Equipe Chimie des Polymères, Institut Parisien de Chimie Moléculaire, Sorbonne Université, CNRS, F-75005 Paris, France; University of Evry, F-91025 Evry Cedex, France*

Pascal Martin − *Université Paris Cité, ITODYS, UMR 7086 CNRS, F-75205 Paris Cedex 13, France;* orcid.org/0000-0003-1010-8421

Fabien Montel − *Laboratoire de Physique, Université Lyon, ENS de Lyon, CNRS, F-69342 Lyon, France;* orcid.org/0000-0001-5430-864X

Complete contact information is available at:
https://pubs.acs.org/10.1021/acsanm.3c02379

Author Contributions

All authors have given approval to the final version of the manuscript.

Notes

The authors declare no competing financial interest.

ABBREVIATIONS

POx, Poly(2-alkyl-2-oxazoline); PMeOx, Poly(2-methyl-2-oxazoline); PnPrOx, Poly(n-propyl-2-oxazoline); ITO, Indium tin oxide; THF, Tetrahydrofuran; AuNPs, Gold nanoparticles; SEM, Scanning electron microscopy; XPS, X-ray photoelectron spectroscopy; AFM, Atomic force microscopy; CA, Contact angle; CV, Cyclic voltammogram; LSPR, Localized Surface Plasmon Resonance

REFERENCES

(1) Wang, D.; Bierwagen, G. P. Sol-Gel Coatings on Metals for Corrosion Protection. *Prog. Org. Coatings* **2009**, *64* (4), 327−338.

(2) Montemor, M. F. Functional and Smart Coatings for Corrosion Protection: A Review of Recent Advances. *Surf. Coat. Technol.* **2014**, *258*, 17−37.

(3) Santos, L.; Martin, P.; Ghilane, J.; Lacaze, P.; Lacroix, J.-C. Micro/Nano-Structured Polypyrrole Surfaces on Oxidizable Metals as Smart Electroswitchable Coatings. *ACS Appl. Mater. Interfaces* **2013**, *5* (20), 10159−10164.

(4) Nath, N.; Chilkoti, A. Creating "Smart" Surfaces Using Stimuli Responsive Polymers. *Adv. Mater.* **2002**, *14* (17), 1243−1247.

(5) Xia, F.; Zhu, Y.; Feng, L.; Jiang, L. Smart Responsive Surfaces Switching Reversibly between Super-Hydrophobicity and Super-Hydrophilicity. *Soft Matter* **2009**, *5* (2), 275−281.

(6) Nguyen, V.-Q.; Schaming, D.; Martin, P.; Lacroix, J.-C. Highly Resolved Nanostructured PEDOT on Large Areas by Nanosphere Lithography and Electrodeposition. *ACS Appl. Mater. Interfaces* **2015**, *7* (39), 21673−21681.

(7) Stuart, M. A. C.; Huck, W. T. S.; Genzer, J.; Müller, M.; Ober, C.; Stamm, M.; Sukhorukov, G. B.; Szleifer, I.; Tsukruk, V. V.; Urban, M.; Winnik, F.; Zauscher, S.; Luzinov, I.; Minko, S. Emerging Applications of Stimuli-Responsive Polymer Materials. *Nat. Mater.* **2010**, *9* (2), 101−113.

(8) Wei, T.; Tang, Z.; Yu, Q.; Chen, H. Smart Antibacterial Surfaces with Switchable Bacteria-Killing and Bacteria-Releasing Capabilities. *ACS Appl. Mater. Interfaces* **2017**, *9* (43), 37511−37523.

(9) Slowing, I.; Trewyn, B. G.; Lin, V. S.-Y. Effect of Surface Functionalization of MCM-41-Type Mesoporous Silica Nanoparticles on the Endocytosis by Human Cancer Cells. *J. Am. Chem. Soc.* **2006**, *128* (46), 14792−14793.

(10) Pelaz, B.; Del Pino, P.; Maffre, P.; Hartmann, R.; Gallego, M.; Rivera-Fernández, S.; De La Fuente, J. M.; Nienhaus, G. U.; Parak, W. J. Surface Functionalization of Nanoparticles with Polyethylene Glycol: Effects on Protein Adsorption and Cellular Uptake. *ACS Nano* **2015**, *9* (7), 6996−7008.

(11) Love, J. C.; Estroff, L. A.; Kriebel, J. K.; Nuzzo, R. G.; Whitesides, G. M. Self-Assembled Monolayers of Thiolates on Metals as a Form of Nanotechnology. *Chem. Rev.* **2005**, *105* (4), 1103−1169.

(12) Ruckenstein, E.; Li, Z. F. Surface Modification and Functionalization through the Self-Assembled Monolayer and Graft Polymerization. *Adv. Colloid Interface Sci.* **2005**, *113* (1), 43−63.

(13) Everett, W. R.; Fritsch-Faules, I. Factors That Influence the Stability of Self-Assembled Organothiols on Gold under Electrochemical Conditions. *Anal. Chim. Acta* **1995**, *307* (2), 253−268.

(14) Allara, D. L.; Parikh, A. N.; Rondelez, F. Evidence for a Unique Chain Organization in Long Chain Silane Monolayers Deposited on Two Widely Different Solid Substrates. *Langmuir* **1995**, *11* (7), 2357−2360.

(15) Soler-Illia, G. J. D. A. A.; Sanchez, C.; Lebeau, B.; Patarin, J. Chemical Strategies to Design Textured Materials: From Microporous and Mesoporous Oxides to Nanonetworks and Hierarchical Structures. *Chem. Rev.* **2002**, *102* (11), 4093−4138.

(16) Pinson, J.; Podvorica, F. Attachment of Organic Layers to Conductive or Semiconductive Surfaces by Reduction of Diazonium Salts. *Chem. Soc. Rev.* **2005**, *34* (5), 429−439.

(17) Bélanger, D.; Pinson, J. Electrografting: A Powerful Method for Surface Modification. *Chem. Soc. Rev.* **2011**, *40* (7), 3995.

(18) Bahr, J. L.; Yang, J.; Kosynkin, D. V.; Bronikowski, M. J.; Smalley, R. E.; Tour, J. M. Functionalization of Carbon Nanotubes by Electrochemical Reduction of Aryl Diazonium Salts: A Bucky Paper Electrode. *J. Am. Chem. Soc.* **2001**, *123* (27), 6536−6542.

(19) Bouriga, M.; Chehimi, M. M.; Combellas, C.; Decorse, P.; Kanoufi, F.; Deronzier, A.; Pinson, J. Sensitized Photografting of Diazonium Salts by Visible Light. *Chem. Mater.* **2013**, *25* (1), 90−97.

(20) Nguyen, V. Q.; Ai, Y.; Martin, P.; Lacroix, J. C. Plasmon-Induced Nanolocalized Reduction of Diazonium Salts. *ACS Omega* **2017**, *2* (5), 1947−1955.

(21) Bastide, M.; Gam-Derouich, S.; Lacroix, J.-C. Long-Range Plasmon-Induced Anisotropic Growth of an Organic Semiconductor between Isotropic Gold Nanoparticles. *Nano Lett.* **2022**, *22* (10), 4253−4259.

(22) Adenier, A.; Combellas, C.; Kanoufi, F.; Pinson, J.; Podvorica, F. I. Formation of Polyphenylene Films on Metal Electrodes by Electrochemical Reduction of Benzenediazonium Salts. *Chem. Mater.* **2006**, *18* (8), 2021−2029.

(23) Santos, L.; Ghilane, J.; Lacroix, J. C. Formation of Mixed Organic Layers by Stepwise Electrochemical Reduction of Diazonium Compounds. *J. Am. Chem. Soc.* **2012**, *134* (12), 5476−5479.

(24) Bousquet, A.; Ceccato, M.; Hinge, M.; Pedersen, S. U.; Daasbjerg, K. Redox Grafting of Diazotated Anthraquinone as a Means of Forming Thick Conducting Organic Films. *Langmuir* **2012**, *28* (2), 1267−1275.

(25) Nguyen, Q. V.; Martin, P.; Frath, D.; Della Rocca, M. L.; Lafolet, F.; Bellinck, S.; Lafarge, P.; Lacroix, J.-C. Highly Efficient Long-Range Electron Transport in a Viologen-Based Molecular Junction. *J. Am. Chem. Soc.* **2018**, *140* (32), 10131−10134.

(26) Jousselme, B.; Bidan, G.; Billon, M.; Goyer, C.; Kervella, Y.; Guillerez, S.; Hamad, E. A.; Goze-Bac, C.; Mevellec, J.-Y. Y.; Lefrant, S. One-Step Electrochemical Modification of Carbon Nanotubes by Ruthenium Complexes via New Diazonium Salts. *J. Electroanal. Chem.* **2008**, *621* (2), 277−285.

(27) Combellas, C.; Kanoufi, F.; Pinson, J.; Podvorica, F. I. Sterically Hindered Diazonium Salts for the Grafting of a Monolayer on Metals. *J. Am. Chem. Soc.* **2008**, *130* (27), 8576−8577.

(28) Frath, D.; Nguyen, V. Q.; Lafolet, F.; Martin, P.; Lacroix, J.-C. Electrografted Monolayer Based on a Naphthalene Diimide-Ruthenium Terpyridine Complex Dyad: Efficient Creation of Large-Area Molecular Junctions with High Current Densities. *Chem. Commun.* **2017**, *53* (80), 10997−11000.

(29) Leroux, Y. R.; Fei, H.; Noël, J.-M.; Roux, C.; Hapiot, P. Efficient Covalent Modification of a Carbon Surface: Use of a Silyl Protecting Group To Form an Active Monolayer. *J. Am. Chem. Soc.* **2010**, *132* (40), 14039−14041.

(30) Fontaine, O.; Ghilane, J.; Martin, P.; Lacroix, J.-C.; Randriamahazaka, H. Ionic Liquid Viscosity Effects on the Functionalization of Electrode Material through the Electroreduction of Diazonium. *Langmuir* **2010**, *26* (23), 18542−18549.

(31) Menanteau, T.; Levillain, E.; Breton, T. Electrografting via Diazonium Chemistry: From Multilayer to Monolayer Using Radical Scavenger. *Chem. Mater.* **2013**, *25* (14), 2905−2909.

(32) Breton, T.; Downard, A. J. Controlling Grafting from Aryldiazonium Salts: A Review of Methods for the Preparation of Monolayers. *Aust. J. Chem.* **2017**, *70* (9), 960−972.

(33) Pichereau, L.; López, I.; Cesbron, M.; Dabos-Seignon, S.; Gautier, C.; Breton, T. Controlled Diazonium Electrografting Driven by Overpotential Reduction: A General Strategy to Prepare Ultrathin Layers. *Chem. Commun.* **2019**, *55* (4), 455−457.

(34) Milner, S. T. Polymer Brushes. *Science.* **1991**, *251* (4996), 905−914.

(35) Barbey, R.; Lavanant, L.; Paripovic, D.; Schuwer, N.; Sugnaux, C.; Tugulu, S.; Klok, H.-A. Polymer Brushes via Surface-Initiated Controlled Radical Polymerization: Synthesis, Characterization, Properties, and Applications. *Chem. Rev.* **2009**, *109* (11), 5437−5527.

(36) Edmondson, S.; Osborne, V. L.; Huck, W. T. S. Polymer Brushes via Surface-Initiated Polymerizations. *Chem. Soc. Rev.* **2004**, *33* (1), 14−22.

(37) Chang, Y.; Ko, C.-Y.; Shih, Y.-J.; Quémener, D.; Deratani, A.; Wei, T.-C.; Wang, D.-M.; Lai, J.-Y. *J. Membr. Sci.* **2009**, *345*, 160−169.

(38) Xu, X.; Wang, Q.; Chang, Y.; Zhang, Y.; Peng, H.; Whittaker, A. K.; Fu, C. Antifouling and Antibacterial Surfaces Grafted with Sulfur Containing Copolymers. *ACS Appl. Mater. Interfaces* **2022**, *14*, 41400−41411.

(39) Suma, M. S.; Basheer, R.; Sreelekshmy, B. R.; Vipinlal, V.; Sha, M. A.; Jineesh, P.; Krishnan, A.; Archana, S. R.; Saji, V. S.; Shibli, S. M. A. *Pseudomonas putida* RSS biopassivation of mild steel for long

term corrosion inhibition. *International Biodeterioration & Biodegradation* **2019**, *137*, 59−67.

(40) Linder, V.; Verpoorte, E.; Thormann, W.; de Rooij, N. F.; Sigrist, H. Surface Biopassivation of Replicated Poly-(dimethylsiloxane) Microfluidic Channels and Application to Heterogeneous Immunoreaction with On-Chip Fluorescence Detection. *Anal. Chem.* **2001**, *73*, 4181−4189.

(41) Mahouche-Chergui, S.; Gam-Derouich, S.; Mangeney, C.; Chehimi, M. M. Aryl Diazonium Salts: A New Class of Coupling Agents for Bonding Polymers, Biomacromolecules and Nanoparticles to Surfaces. *Chem. Soc. Rev.* **2011**, *40* (7), 4143−4166.

(42) Mo, F.; Qiu, D.; Zhang, L.; Wang, J. Recent Development of Aryl Diazonium Chemistry for the Derivatization of Aromatic Compounds. *Chem. Rev.* **2021**, *121* (10), 5741−5829.

(43) Gam-Derouich, S.; Ngoc Nguyen, M.; Madani, A.; Maouche, N.; Lang, P.; Perruchot, C.; Chehimi, M. M. Aryl Diazonium Salt Surface Chemistry and ATRP for the Preparation of Molecularly Imprinted Polymer Grafts on Gold Substrates. *Surf. Interface Anal.* **2010**, *42* (6−7), 1050−1056.

(44) Gam-Derouich, S.; Carbonnier, B.; Turmine, M.; Lang, P.; Jouini, M.; Ben Hassen-Chehimi, D.; M. Chehimi, M. Electrografted Aryl Diazonium Initiators for Surface-Confined Photopolymerization: A New Approach to Designing Functional Polymer Coatings. *Langmuir* **2010**, *26* (14), 11830−11840.

(45) Gam-Derouich, S.; Mahouche-Chergui, S.; Turmine, M.; Piquemal, J.-Y.; Hassen-Chehimi, D. B.; Omastová, M.; Chehimi, M. M. A Versatile Route for Surface Modification of Carbon, Metals and Semi-Conductors by Diazonium Salt-Initiated Photopolymerization. *Surf. Sci.* **2011**, *605* (21−22), 1889−1899.

(46) Adenier, A.; Cabet-Deliry, E.; Lalot, T.; Pinson, J.; Podvorica, F. Attachment of Polymers to Organic Moieties Covalently Bonded to Iron Surfaces. *Chem. Mater.* **2002**, *14* (11), 4576−4585.

(47) Mahouche, S.; Mekni, N.; Abbassi, L.; Lang, P.; Perruchot, C.; Jouini, M.; Mammeri, F.; Turmine, M.; Romdhane, H. B.; Chehimi, M. M. Tandem Diazonium Salt Electroreduction and Click Chemistry as a Novel, Efficient Route for Grafting Macromolecules to Gold Surface. *Surf. Sci.* **2009**, *603* (21), 3205−3211.

(48) Squillace, O.; Esnault, C.; Pilard, J.-F.; Brotons, G. Grafting Commercial Surfactants (Brij, CiEj) and PEG to Electrodes via Aryldiazonium Salts. *ACS Appl. Mater. Interfaces* **2017**, *9* (48), 42313−42326.

(49) Romero-Ben, E.; Cid, J. J.; Assali, M.; Fernández-García, E.; Wellinger, R. E.; Khiar, N. Surface Modulation of Single-Walled Carbon Nanotubes for Selective Bacterial Cell Agglutination. *Int. J. Nanomedicine* **2019**, *14*, 3245−3263.

(50) Du, H.; de Oliveira, F. A.; Albuquerque, L. J. C.; Tresset, G.; Pavlova, E.; Huin, C.; Guégan, P.; Giacomelli, F. C. Polyglycidol-Stabilized Nanoparticles as a Promising Alternative to Nanoparticle PEGylation: Polymer Synthesis and Protein Fouling Considerations. *Langmuir* **2020**, *36* (5), 1266−1278.

(51) Sun, M.; Qiu, H.; Su, C.; Shi, X.; Wang, Z.; Ye, Y.; Zhu, Y. Solvent-Free Graft-From Polymerization of Polyvinylpyrrolidone Imparting Ultralow Bacterial Fouling and Improved Biocompatibility. *ACS Appl. Bio Mater.* **2019**, *2* (9), 3983−3991.

(52) Utrata-Wesołek, A.; Wałach, W.; Bochenek, M.; Trzebicka, B.; Anioł, J.; Sieroń, A. L.; Kubacki, J.; Dworak, A. Branched polyglycidol and its derivatives grafted-from poly(ethylene terephthalate) and silica as surfaces that reduce protein fouling. *Eur. Polym. J.* **2018**, *105*, 313−322.

(53) Le, D.; Wagner, F.; Takamiya, M.; Hsiao, I. L.; Gil Alvaradejo, G.; Strähle, U.; Weiss, C.; Delaittre, G. Straightforward access to biocompatible poly(2-oxazoline)-coated nanomaterials by polymerization-induced self-assembly. *Chem. Commun.* **2019**, *55*, 3741−3744.

(54) Leiske, M. N. Poly(2-oxazoline)-derived star-shaped polymers as potential materials for biomedical applications: A review. *Eur. Polym. J.* **2023**, *185*, 111832.

(55) Morgese, G.; Benetti, E. M. Polyoxazoline biointerfaces by surface grafting. *Eur. Polym. J.* **2017**, *88*, 470−485.

H

(56) Jordan, R.; Ulman, A. Surface Initiated Living Cationic Polymerization of 2-Oxazolines. *J. Am. Chem. Soc.* **1998**, *120* (2), 243−247.

(57) Jordan, R.; West, N.; Ulman, A.; Chou, Y.-M.; Nuyken, O. Nanocomposites by Surface-Initiated Living Cationic Polymerization of 2-Oxazolines on Functionalized Gold Nanoparticles. *Macromolecules* **2001**, *34* (6), 1606−1611.

(58) Trachsel, L.; Romio, M.; Grob, B.; Zenobi-Wong, M.; Spencer, N. D.; Ramakrishna, S. N.; Benetti, E. M. Functional Nanoassemblies of Cyclic Polymers Show Amplified Responsiveness and Enhanced Protein-Binding Ability. *ACS Nano* **2020**, *14* (8), 10054−10067.

(59) Yan, W.; Divandari, M.; Rosenboom, J.-G.; Ramakrishna, S. N.; Trachsel, L.; Spencer, N. D.; Morgese, G.; Benetti, E. M. Design and Characterization of Ultrastable, Biopassive and Lubricious Cyclic Poly(2-Alkyl-2-Oxazoline) Brushes. *Polym. Chem.* **2018**, *9* (19), 2580−2589.

(60) Ali, M. W.; Muhammad, Z.; Jia, Q.; Li, L.; Saleem, M.; Siddiq, M.; Chen, Y. Synthesis of cyclic poly(2-ethyl-2-oxazoline) with a degradable disulfide bond. *Polym. Chem.* **2020**, *11*, 4164−4171.

(61) Pereira, G.; Huin, C.; Morariu, S.; Bennevault-Celton, V.; Guégan, P. Synthesis of Poly(2-methyl-2-oxazoline) Star Polymers with a *β*-cyclodextrine Core. *Aust. J. Chem.* **2012**, *65* (8), 1145−1155.

(62) Loukotová, L.; Konefał, R.; Venclíková, K.; Machová, D.; Janoušková, O.; Rabyk, M.; Netopilík, M.; Mázl Chánová, E.; Štěpánek, P.; Hrubý, M. Hybrid thermoresponsive graft constructs of fungal polysaccharide *β*-glucan: physico-chemical and immunomodulatory properties. *Eur. Polym. J.* **2018**, *106*, 118−127.

(63) Pospisilova, A.; Filippov, S. K.; Bogomolova, A.; Turner, S.; Sedlacek, O.; Matushkin, N.; Cernochova, Z.; Stepanek, P.; Hruby, M. Glycogen-graft-poly(2-alkyl-2-oxazolines) − the new versatile biopolymer-based thermoresponsive macromolecular toolbox. *RSC Adv.* **2014**, *4*, 61580−61588.

(64) Hoogenboom, R.; Thijs, H. M. L.; Jochems, M. J. H. C.; van Lankvelt, B. M.; Fijten, M. W. M.; Schubert, U. S. Tuning the LCST of poly(2-oxazoline)s by varying composition and molecular weight: alternatives to poly(*N*-isopropylacrylamide)? *Chem. Commun.* **2008**, 5758−5760.

(65) Hoogenboom, R. Poly(2-oxazoline)s: Alive and Kicking. *Macromol. Chem. Phys.* **2007**, *208* (1), 18−25.

(66) Baranton, S.; Bélanger, D. In Situ Generation of Diazonium Cations in Organic Electrolyte for Electrochemical Modification of Electrode Surface. *Electrochim. Acta* **2008**, *53* (23), 6961−6967.

(67) Amatore, C.; Savéant, J. M.; Tessier, D. Charge transfer at partially blocked surfaces: A model for the case of microscopic active and inactive sites. *Journal of electroanalytical chemistry and interfacial electrochemistry* **1983**, *147* (1−2), 39−51.

(68) Santos, L.; Ghilane, J.; Lacroix, J.-C. Surface Patterning Based on Nanosphere Lithography and Electroreduction of in Situ Generated Diazonium Cation. *Electrochem. commun.* **2012**, *18*, 20−23.

(69) Schaming, D.; Nguyen, V.-Q.; Martin, P.; Lacroix, J.-C. Tunable Plasmon Resonance of Gold Nanoparticles Functionalized by Electroactive Bisthienylbenzene Oligomers or Polythiophene. *J. Phys. Chem. C* **2014**, *118* (43), 25158−25166.

(70) Bennevault-Celton, V.; Urbach, A.; Martin, O.; Pichon, C.; Guégan, P.; Midoux, P. Supramolecular Assemblies of Histidinylated *α*-Cyclodextrin in the Presence of DNA Scaffold during CDplexes Formation. *Bioconjugate Chem.* **2011**, *22* (12), 2404−2414.

(71) Rassou, S.; Illy, N.; Tezgel, O.; Guégan, P. ″Anionic ring opening polymerization of *N*-glycidylphthalimide: combination of phosphazene base and activated monomer mechanism″. *Journal of Polymer Science: Polymer Chemistry* **2018**, *56*, 1091−1099.

(72) Stockhausen, V.; Trippe-Allard, G.; Van Quynh, N.; Ghilane, J.; Lacroix, J.-C. Grafting *π*-Conjugated Oligomers Incorporating 3, 4-Ethylenedioxythiophene (EDOT) and Thiophene Units on Surfaces by Diazonium Electroreduction. *J. Phys. Chem. C* **2015**, *119* (33), 19218−19227.